iScience

CellPress
OPEN ACCESS

Article

The spatiotemporal extent of the Green Sahara during the last glacial period

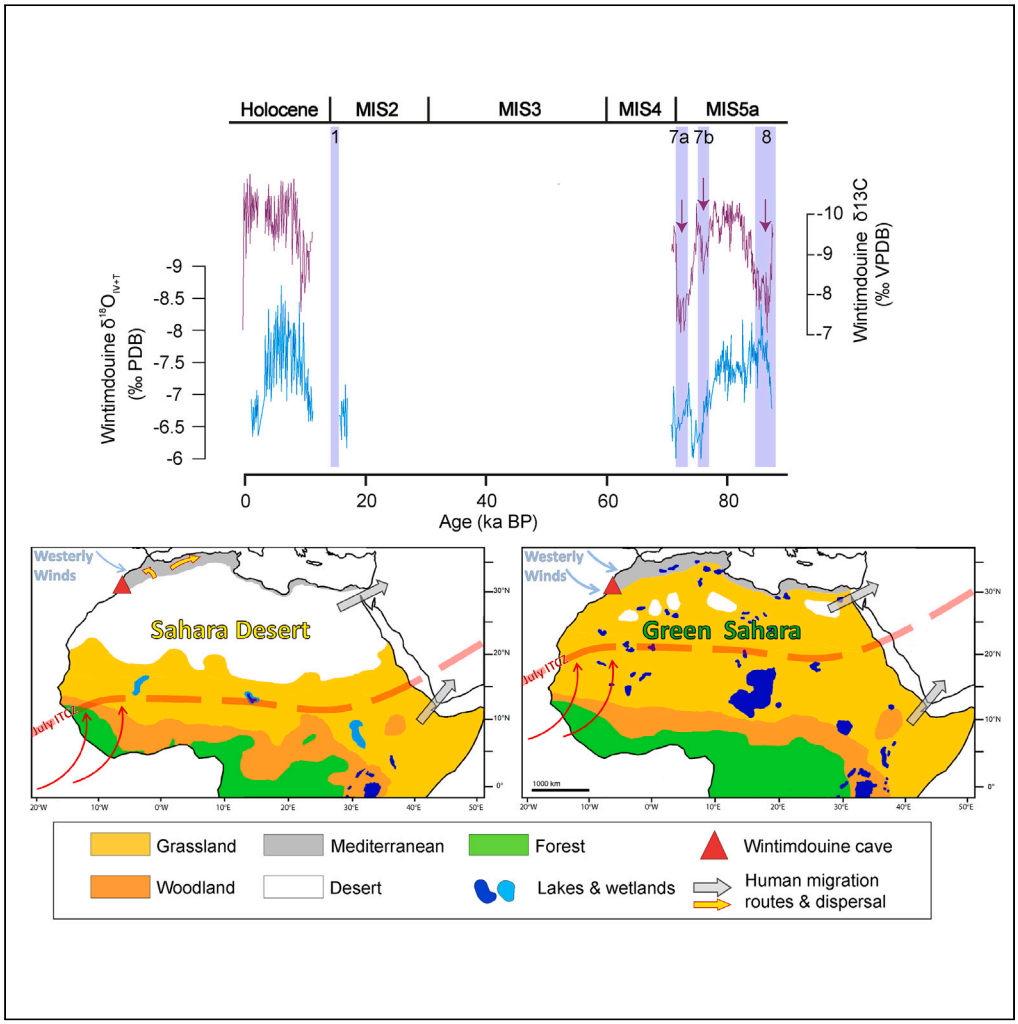

Yassine Ait Brahim, Lijuan Sha, Jasper A. Wassenburg, Khalil Azennoud, Hai Cheng, Francisco W. Cruz, Lhoussaine Bouchaou

yassine.aitbrahim@um6p.ma

Highlights

New speleothem data from NW Africa reveal Green Sahara conditions during MIS5a

Triple oxygen data reveal enhanced winter precipitation during MIS5a

Abrupt cooling events resulted in dry conditions in NW Africa

Climate deterioration and decline in human density during MIS5-4 transition

Ait Brahim et al., iScience 26, 107018
July 21, 2023
https://doi.org/10.1016/j.isci.2023.107018

iScience

CellPress
OPEN ACCESS

Article

The spatiotemporal extent of the Green Sahara during the last glacial period

Yassine Ait Brahim,[1,7,*] Lijuan Sha,[2] Jasper A. Wassenburg,[3,4] Khalil Azennoud,[1] Hai Cheng,[2] Francisco W. Cruz,[5] and Lhoussaine Bouchaou[1,6]

SUMMARY

The Sahara Desert, one of today's most inhospitable environments, has known periods of enhanced precipitation that supported pre-historic humans. However, the Green Sahara timing and moisture sources are not well known due to limited paleoclimate information. Here, we present a multi-proxy ($\delta^{18}O$, $\delta^{13}C$, $\Delta^{17}O$, and trace elements) speleothem-based climate record from Northwest (NW) Africa. Our data document two Green Sahara periods during Marine Isotope Stage (MIS) 5a and the Early to Mid-Holocene. Consistency with paleoclimate records across North Africa highlights the east-west geographical extent of the Green Sahara, whereas millennial-scale North Atlantic cooling (Heinrich) events consistently resulted in drier conditions. We demonstrate that an increase in westerly-originating winter precipitation during MIS5a resulted in favorable environmental conditions. The comparison of paleoclimate data with local archaeological sequences highlights the abrupt climate deterioration and the decline in human density in NW Africa during the MIS5-4 transition, which suggests climate-forced dispersals of populations, with possible implications for pathways into Eurasia.

INTRODUCTION

Freshwater supply and favorable climate conditions have always been major controls on the survival of human populations. In the tropical and subtropical regions of the African continent, changes in climate dynamics resulted in major oscillations of humid and dry periods. Archeological and paleoclimate evidence shows that what is nowadays known as the Sahara Desert was almost entirely vegetated and covered by rivers and mega-lakes during the "Green Sahara" periods. The increase in rainfall over the Sahara resulted from an orbitally forced increase in the northern hemisphere summer insolation and the resultant strengthening of the African monsoon. Paleoclimate data suggest that the northern fringe of the African monsoon could have reached as far north as ~31°N.[1,2] This observation is also supported by model simulations that include vegetation changes and dust reduction during this period.[3]

Furthermore, proxy and modeling results show that the strengthening of the North African monsoon and the northward displacement of the intertropical convergence zone (ITCZ) is in phase with enhanced precipitation in the Mediterranean region during precession minima, which cause high seasonal contrasts[4,5] (summer insolation maxima and winter insolation minima). Reduced northern hemisphere winter insolation induces low latitude cooling leading to a reduced meridional temperature gradient. This causes a southward shift of the Hadley and Ferrell cells and the westerlies, associated with increased precipitation in the Mediterranean.[4] As a result, the areas affected by the northern fringe of the African monsoon (i.e., the Mediterranean region of North Africa) could also be influenced by winter precipitation.[5] Such a dual-season precipitation system, resulting from the combined effect of two seasonally distinct rainfall regimes, could have contributed to a reduction in the width of the North African Sahara Desert.

In addition to orbital-scale variability, Earth's climate was punctuated by abrupt and widespread millennial-scale fluctuations in northern hemisphere temperature,[6] which have been linked to changes in the strength of the Atlantic meridional overturning circulation (AMOC) and the heat distribution between the northern and southern hemispheres. Furthermore, during the northern hemisphere summer, cooling events (i.e., Heinrich events [HEs]/Greenland stadials) induce latitudinal shifts of the ITCZ toward a more southward

[1]International Water Research Institute, Mohammed VI Polytechnic University, Benguerir, Morocco

[2]Institute of Global Environmental Change, Xi'an Jiaotong Uniersity, Xi'an, China

[3]Center for Climate Physics, Institute for Basic Science, Busan, 46241, Republic of Korea

[4]Pusan National University, Busan, 46241, Republic of Korea

[5]Instituto de Geociências, University of Sao Paulo, Sao Paulo, Brazil

[6]Laboratory of Applied Geology and Geo-Environmental, Ibn Zohr University, Agadir, Morocco

[7]Lead contact

*Correspondence: yassine.aitbrahim@um6p.ma

https://doi.org/10.1016/j.isci.2023.107018

position, resulting in weaker monsoons over the northern hemisphere[7] and stronger monsoons over the Southern Hemisphere.[8] HEs are also associated with a southward shift of the oceanic thermal front. The jet stream follows the oceanic thermal front and controls the position of the westerly storm track, potentially affecting the amount of winter precipitation received in the Mediterranean.[9]

The Early to Mid-Holocene humid period in the Sahara is one among many Green Sahara periods when enhanced humidity, ample vegetation, and riparian ecosystems were more favorable for human subsistence.[10–13] Before 100 ka BP, fossils of sub-Saharan animals (rhinos, giraffes, and hippos) at North African sites suggest environment amelioration that ecologically connects North Africa to the rest of the continent. The Green Sahara conditions might have supported the early human populations that were present in North Africa since 300 ka BP, as shown by fossil finds from Jebel Irhoud in Morocco.[14] Central questions have been proposed about the potential role of climate in "pulsing" early and late dispersals of humans outside Africa. Robust climate reconstructions allow us to provide new insights into the climate conditions that might have caused the dispersals of anatomically modern humans (AMHs) in and out of Africa. The most common hypothesis is that the African monsoon climate nourished the Sahara Desert, creating corridors that could be used to move outside of the African continent during the Green Sahara periods.[15] However, a different hypothesis suggests that different AMH populations *lived in* isolated refugia, and they might have been "pushed" out of Africa as a survival pulse,[16] probably via corridors (e.g., the Nile River, coastlines). New paleoclimate evidence also indicates a role in increased winter precipitation in Northern Africa, in addition to a northward shift of the African monsoon, to contribute to the Green Sahara conditions.[4,5]

Furthermore, there has been considerable debate about the potential factors (including the downstream effects of climate on environmental conditions) behind the cultural evolution of the region in general and the emergence of modern human behavior through different timescales.[17,18] Archaeological evidence suggests that the cultural change of North African humans might have been linked to climate variability.[19] The Middle Stone Age (MSA) in the Maghreb is typically described as consisting of two stone cultural industries, the "Mousterian" and "Aterian", *a priori* distinguishable by the absence or presence of tanged pieces, respectively,[20] although there is some debate concerning the "Aterian" term when applicable to entire North Africa.[19] While the oldest Aterian occupation is dated to about 145 ka Before the Present (BP) in Ifri n'Ammar in Morocco,[21] the number of Aterian sites increased during Marine Isotope Stage (MIS) 5 and continued in the Maghreb until ~30 ka BP.[22] Besides, several archaeological sites in Morocco highlighted the point that the intense Aterian occupations during MIS5 are marked by periods where archeological sterile layers and/or MSA layers without tanged tools took place,[23,24] presumably ascribed to climate changes (e.g., Jacobs et al.[25]). Interestingly, intense beadwork innovation during later MIS5 substages using similar marine shells was reported in several remote sites (e.g., Maghreb, South Africa), suggesting organized networks among remote groups, but sharply decreased afterward.[26] To date, while archaeological evidence of human occupation density and behavior changes in Northwest (NW) Africa, and especially in Morocco, at the MIS5-4 transition has been roughly raised, the potential effect of climate, and hence the Green Sahara extension phases, still needs to be assessed.

Here, we discuss a new high-resolution and precisely dated multi-proxy speleothem record based on stable isotopes ($\delta^{18}O$ and $\delta^{13}C$) from three stalagmites from Wintimdouine cave (Figure S1) (30.68°N, 9.34°W, 1200 m.a.s.l.) in Southwest (SW) Morocco (Figure 1). Our record is also supported by speleothem carbonate $\Delta^{17}O$ and trace element data. The new Wintimdouine cave record is then compared to paleoclimate and archaeological evidence in order to provide new insights into the climate history of and potential human/climate interactions in NW Africa, a region where high-resolution climate archives are still lacking, so as other speleothem studies have revealed from other regions in Africa (e.g., Bar-Matthews et al.[27]). We also used our climate reconstructions to test the presence of large-scale atmospheric teleconnections linking hydro-climate changes in the sub-Saharan regions with the northern hemisphere abrupt events and the low-latitude African monsoon systems.

RESULTS

Age model of speleothem records

^{230}Th dating shows that stalagmites Wintimdouine (WIN)1 and WIN3 span the periods 5.8–5.5 and 11.5–0.2 ka BP, respectively.[1,28] A growth hiatus was identified in stalagmite WIN3 from 4 to 1.9 ka BP. Here we present new ^{230}Th dating results which show that stalagmite WIN1 also spans an older period from 17.4 to 16.3

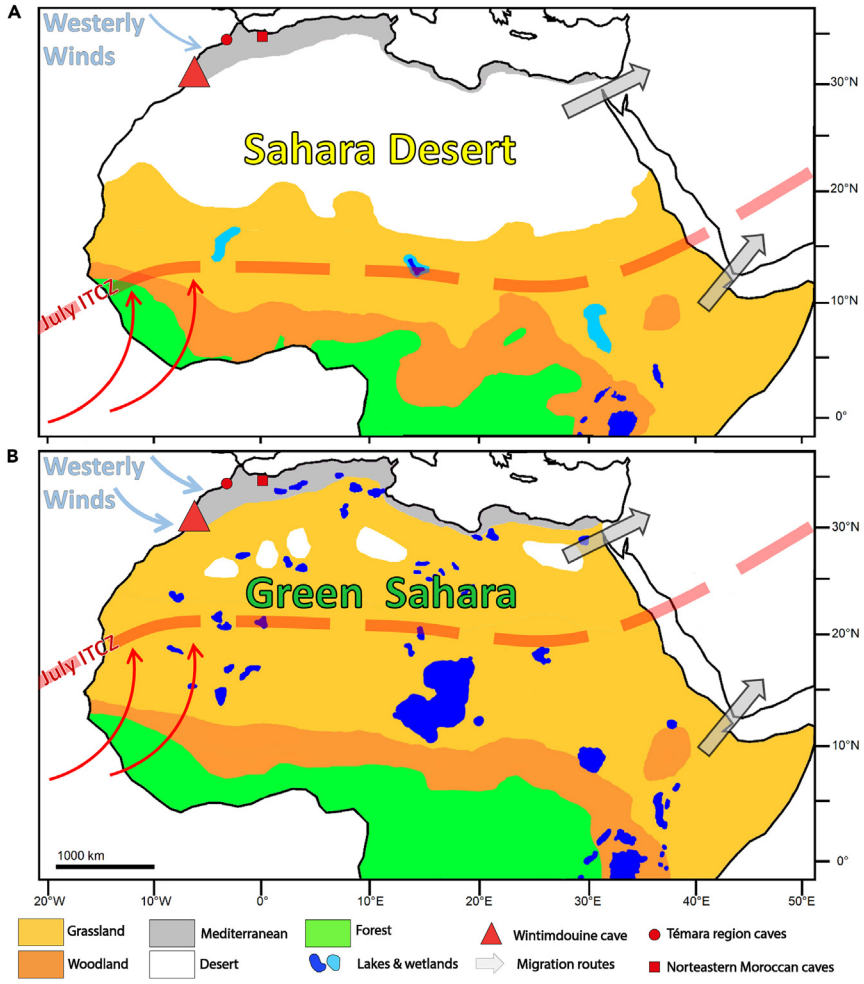

Figure 1. Conceptual model of desert and green Sahara conditions

Conceptual model of the desert (A) and Green (B) Sahara conditions, with typical positions of the Westerly winds and July ITCZ. The spatial extent of different vegetation types and the positions of lakes and wetlands were adapted from Larrasoaña et al.[12] The concept of Green Sahara illustrates mega-lakes with no ecological barriers isolating NW Africa from the rest of the continent. The location of Wintimdouine cave where speleothem samples were collected for this study (red triangle). The gray arrows indicate the most suggested routes for modern humans' dispersal out of Africa through the Nile valley and Bab Al Mandab.

ka BP, whereas stalagmite WIN15 spans the period from 87.2 to 71.7 ka BP (Figure S2) Table S1). The age-depth model of each stalagmite was constructed (Figure S3) using the StalAge algorithm.[29]

Interpretation of Wintimdouine speleothem isotopes ($\delta^{18}O$ and $\delta^{13}C$)

Previous cave monitoring showed that the stable isotope composition of drip water samples from Wintimdouine is consistent with the isotope signal of rainwater.[30] Furthermore, Sha et al.[1] showed that the WIN3 $\delta^{18}O$ record replicates with other speleothem records from Wintimdouine, as well as Ifoulki cave in Southwestern Morocco,[31] during their common growth periods. This suggests that the $\delta^{18}O$ variability of Wintimdouine cave speleothems reflects the overall variability of $\delta^{18}O$ in precipitation ($\delta^{18}O_p$) above the cave.

The $\delta^{18}O_p$, reflected by our speleothem $\delta^{18}O$, can be influenced by several climate and environmental factors. In the cave region, an inverse correlation between rainfall amount and $\delta^{18}O$ was found significant.[31,32] This is especially valid for the present-day climate and the late Holocene with winter precipitation from the westerlies, dry summers, and no major changes in atmospheric circulation patterns. However, it has been shown that the Wintimdouine cave site also experienced increased summer rainfall with a monsoonal origin

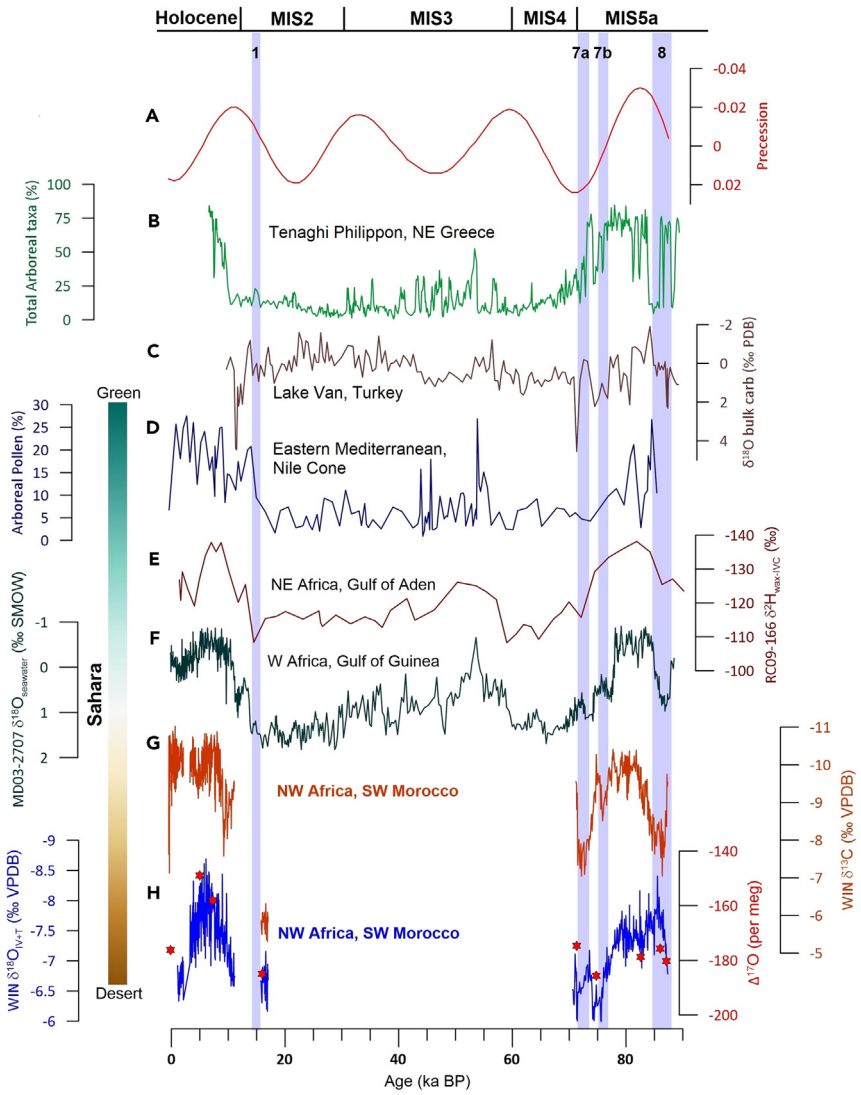

Figure 2. Comparison of the Wintimdouine cave records with regional paleoclimate records

Comparison of the Wintimdouine cave $\delta^{18}O$, $\Delta^{17}O$, and $\delta^{13}C$ records in SW Morocco (G and H) with the (A) Earth's orbital precession,[33] (B) the total arboreal taxa from Tenaghi Philippon in Northeast (NE) Greece,[34] (C) the $\delta^{18}O$ record in bulk carbonates from Lake Van in Turkey,[35] (D) the Arboreal taxa from the Nile cone,[36] (E) the $\delta^{2}H$ record from the Gulf of Aden,[2] and (F) the $\delta^{18}O$ record from the Gulf of Guinea.[7]

during the Early to Mid-Holocene,[1] which was likely associated with enhanced upstream depletion, leading to more negative speleothem $\delta^{18}O$ values (Figure 2H).

The combined $\delta^{18}O$ record of Wintimdouine stalagmites was corrected for global ice volume changes (hereafter $\delta^{18}O_{IV}$) by subtracting 0.008‰ per meter of sea-level change,[37] using the most detailed sea-level data with an independent age model by Grant et al.[38] (Figure S4). Furthermore, northern hemisphere temperature variations during the last glacial period were even larger on millennial timescales due to iceberg-discharge events in the North Atlantic (HEs) and the weakening of the AMOC.[39] Hence, the $\delta^{18}O_{IV}$ variability in the Wintimdouine record might result from a combination of temperature and changes in the proportion of precipitation from the North African summer monsoon and winter westerlies to annual mean $\delta^{18}O_P$. An increased summer monsoon contribution and increased winter precipitation might both lead to more negative $\delta^{18}O_{IV}$, affecting annual mean $\delta^{18}O_p$ in the same way. Since a local temperature reconstruction is lacking in the Wintimdouine cave region, we used surface air temperature from a

LOVECLIM transient climate model run[40] to assess and correct the effect of cave air temperature on the Wintimdouine $\delta^{18}O_{IV}$ on orbital timescales, using the temperature gradient of −0.21‰/°C.[41] We refer to the corrected data hereafter as $\delta^{18}O_{IV+T}$ (Figure S4).

The Wintimdouine $\delta^{13}C$ variability shows a similar long-term trend to $\delta^{18}O_{IV+T}$ with more negative values around 80 ka BP and more positive values around 73 ka BP, suggesting that both proxies respond to the same climate forcing on orbital timescales. Furthermore, we show that a part of the $\delta^{13}C$ variation can be explained by prior calcite precipitation as indicated by the shared variance with WIN15 Mg/Ca and Sr/Ca in a principal-component analysis (STAR Methods; Figure S5, Tables S2 and S3). This suggests that WIN15 $\delta^{13}C$ is a proxy for infiltration combined with fractionation processes related to fluctuating vegetation productivity in response to colder and drier or warmer and wetter conditions, which both force speleothem $\delta^{13}C$ in the same direction.[42]

DISCUSSION

Orbital-scale climate variability

The combined $\delta^{18}O$ record of Wintimdouine stalagmites reveals a large variability on multi-millennial timescales with $\delta^{18}O_{IV+T}$ values ranging from −8.7 to −6‰, whereas two distinctive periods of low $\delta^{18}O_{IV+T}$ values are observed (Figure 2H). The most recent period (from 9 to 4 ka BP) corresponds to the Early to Mid-Holocene humid period in NW Africa,[1] whereas the previous period occurred during the most recent substage of MIS5 (MIS5a). During the Early to Mid-Holocene, paleoclimate data and simulations demonstrate that the African monsoon could reach 31°N in NW Africa.[1–3] The Wintimdouine record suggests that this might also be the case during the warm substage of MIS5a (Figure 2). Humid conditions have indeed prevailed during MIS5, as shown by multiple fossil and paleoclimate datasets representing the African monsoon[10,43] (Figures 2D–2F), specifically during the warm substages of MIS5.[15,44] However, MIS5a coincides with a precession minimum centered around 83 ka BP (Figure 2A), which causes high seasonality in local insolation.[5] While such orbital precession change results in a strong northward extent of the summer monsoon associated with a northward shift of the ITCZ,[45,46] it also increases winter precipitation in the Mediterranean region[4,5] (Figures 2B and 2C). Thus, these two seasonally distinct climate regimes might periodically overlap between 25°N[5] and 31°N[1–3] in North Africa. Furthermore, the range of variability of speleothem $\Delta^{17}O$ values during MIS5a (−175 to −186 per Meg) is within the range of $\Delta^{17}O$ measured during the late Holocene (−176 per Meg), suggesting a westerly-related winter moisture regime in NW Africa during MIS5a.

After MIS5a, the Wintimdouine $\delta^{18}O_{IV+T}$ and $\delta^{13}C$ records show a large shift toward more positive values around the MIS5-4 transition, reaching −6 and −7.1‰ respectively. This shift suggests a significant change in the moisture source and/or the onset of relatively drier conditions in NW Africa which peaked during the MIS5-4 transition. This period coincides with an opposite phase of the orbital precession cycle centered around 73 ka BP (Figure 2A), with increased northern hemisphere winter insolation leading to a reduction of winter precipitation and a decrease in northern hemisphere summer insolation leading to a weakening of the North African monsoon. This would have resulted in the expansion of the Sahara Desert, which is clearly observed in sediment records from the West African coast[7,47] and the Nile fan.[36] The MIS5-4 transition toward drier conditions was also observed in the Mediterranean region, e.g., the sediment records from Lake Van in Turkey[35] and Tenaghi Philippon in NE Greece[34] (Figures 2B and 2C). Both Mediterranean and North African monsoon paleoclimate records show that dry conditions were sustained during MIS4 (71–60 ka BP). MIS3 was characterized by a resumption of humid conditions,[43] which were wetter compared to modern climate conditions, as shown by speleothem records from Libya.[48,49] However, MIS3 was not a Green Sahara period,[2,38] as rainfall was not sufficient to sustain ample vegetation.

The last Green Sahara period occurred during the Early to Mid-Holocene, during which the North African monsoon fringe reached its northernmost extent, as revealed by paleoclimate data from Wintimdouine Cave,[1] marine sediments,[2] and climate simulations.[3] Modeling experiments showed only a slight increase in vegetation and winter rainfall in the Mediterranean region during the Early Holocene.[5] This is also confirmed by comparison with speleothem records from Northern Morocco,[50] which represent winter precipitation throughout the Holocene, and did not show the same Early to Mid-Holocene $\delta^{18}O$ excursion as in Wintimdouine cave speleothems in South Morocco. The $\delta^{18}O_{IV+T}$ variability between a short time interval centered on 17 ka BP and throughout the Holocene is coherent with the $\Delta^{17}O$ values measured in stalagmites WIN1 and WIN3. From 17 to 5.5 ka BP, the $\Delta^{17}O$ and the $\delta^{18}O$ values changed from −185 per Meg

and −5.5‰ to −149 per Meg and −8.2‰ and then returned to −176 per Meg and −6.7‰ during the late Holocene (0.3 ka BP), respectively. Such a large difference in the $\Delta^{17}O$ content (up to 36 per Meg) cannot be attributed to changes in relative humidity conditions at the vapor source alone. Instead, the $\Delta^{17}O$ results highlight a change in the source region of moisture and a potential shift in the climate regime from westerly winter precipitation to North African summer monsoon precipitation.

Response to abrupt climate change in the North Atlantic high latitudes

The Wintimdouine record indicates relatively short and yet large positive $\delta^{18}O$ and $\delta^{13}C$ excursions. The comparison of our data with the robustly dated Northern rim of the Alps (NALPS) speleothem $\delta^{18}O$ record[51] and the North Greenland Ice Core Project (NGRIP) $\delta^{18}O$ record (Figure S6) shows that the millennial peaks observed in the Wintimdouine $\delta^{13}C$ record around 87, 76, 72 and 17 ka BP coincide with the high-latitude HEs HE8, HE7b, HE7a and a period before HE1, respectively, indicating that these correspond to colder and potentially drier periods. Interestingly, the Wintimdouine MIS5 $\delta^{13}C$ variations match the northwest African humidity index and the river runoff record from the Gulf of Guinea (Figure 2F).

The most prominent Green Sahara conditions during MIS5a are associated with Dansgaard-Oeschger interval 21 (DO21), which was preceded and followed by abrupt dry phases[7,47] (HE8; HE7a; HE7b). HEs are stadials during which the African monsoon cannot reach SW Morocco. However, the Wintimdouine MIS5 $\delta^{18}O_{IV+T}$ record shows its most negative values of around −8.4‰ within HE8. The negative $\delta^{18}O$ peak during HE8 is in contrast with other North African monsoon records that show a dry Sahara (Figure 2), ruling out a role for summer precipitation in SW Morocco during this period. This is also confirmed by the limited variability of $\Delta^{17}O$ during the HEs and their similar values as the late Holocene, suggesting that the speleothem $\delta^{18}O$ recorded a winter signal during the HEs. As such, the climate variability observed in the Wintimdouine $\delta^{18}O_{IV+T}$ record within HE8 might be related to a relatively short increase in winter precipitation or temperature variation. Indeed, during HE8 (from 87.8 ka to 86.1 ka BP) and the time period encompassing HE7a and HE7b (76.5–72 ka BP), $\delta^{18}O_{IV+T}$ and $\delta^{13}C$ are significantly negatively correlated ($r = -0.55$, $p < 0.01$, $n = 30$ and $r = -0.56$, $p < 0.001$, $n = 41$, respectively). This inverse correlation between $\delta^{18}O_{IV+T}$ and $\delta^{13}C$ is most likely related to temperature variations. Soil CO_2 $\delta^{13}C$ typically becomes more positive at colder temperatures due to decreasing vegetation productivity.[42] It appears that cooler atmospheric temperatures during HEs forced $\delta^{18}O_P$ to relatively more negative values and that this likely overprinted the effect of cave air temperature on speleothem calcite $\delta^{18}O$. Furthermore, the southward shift of the position of the westerly storm track, associated with the southward shift of the oceanic thermal front during the HEs, did not result in increasing winter precipitation in NW Africa. This might be explained by reduced evaporation due to lower sea surface temperatures[52] (SSTs). Moreover, the short period recorded by stalagmite WIN1, just before HE1, is associated with the most positive $\delta^{13}C$ and $\delta^{18}O_{IV+T}$ values. This clearly shows that SW Morocco experienced relatively dry conditions all year round during this period. Although the Wintimdouine record does not cover HE1, the fact that stalagmite WIN3 stopped growing at the onset of HE1 suggests that HE1 might have been dry as well.

Insights on human/climate interactions

In order to address the question of the downstream effect of climate on AMH behavioral traits and occupation densities in NW Africa, we tentatively compared our data with the well-dated archaeological sequences from Moroccan coastal and inland sites (Figures 3B–3F), regardless of the different temporal resolutions of both two datasets and the considerable age uncertainties of archaeological layers/units. Preliminary archaeological insights from Atlantic coastal sites Témara region (Figures 1 and S1) yielded evidence of intense human occupations with tanged lithics centered at MIS5c and MIS5a and low occupations between 60 and 50 ka BP, separated by archaeologically sterile layers.[25] However, recent timeline models of two extensively excavated sequences, viz. El Mnasra[53] and El Harhoura 2[54] caves, brought some nuances to this direct association. Based on Bayesian-model timelines, the revision of the archaeological sequence of El Mnasra recently carried out by Ben Arous et al.[53] yields some new insights (Figure 3B). Although with a slight decrease upward, intense occupations with abundant Aterian tools and evidence of marine shell use (Nassariidae) and consumption (Patellidae and Mytilidae), along with other interesting behavioral traits (e.g., pigment use, osseous industry), characterize the archaeological units US 8d-6 whose deposition time ranges from MIS5c to MIS4 (Ben Arous et al.,[53] their Figure 8). Considering also the paleoenvironmental readings, these occupations have been tentatively ascribed to MIS5c (US 8d-a) and MIS5a (US7 and 6). In addition, low occupation with the persistent occurrence of *Nassarius* beads in more continental settings (US 5) has been ascribed to MIS4. Besides, phases of Aterian settlements between MIS5c and MIS5a in

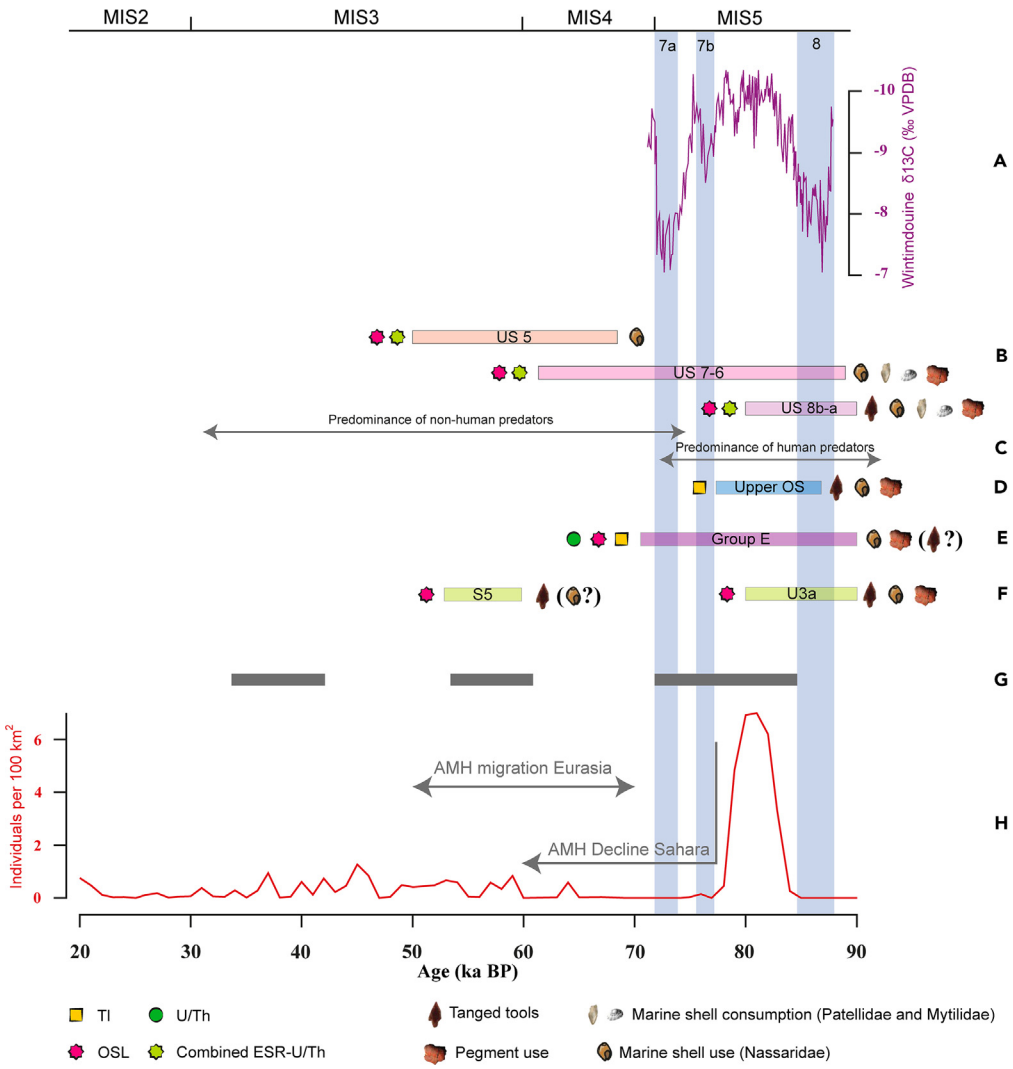

Figure 3. Comparison of the Wintimdouine cave records with archaeological data

Comparison of the Wintimdouine cave $\delta^{13}C$ record in SW Morocco (A) with (B–F) archeological data from Moroccan caves, (G) the regional probability density function of dated sites in NW Africa,[58] and (H) the human density in the NW African Sahara[15] (the region encompassing 28 to 33°N and −10 to 20°E). The archeological data from Moroccan caves encompass (B and C) El Mnasra cave[53,57] from the coastal Témara region, and (D) Ghafas,[59] (E) Ifri n'Ammar cave,[21] (F) Tafolalt[60] and (F) Ghafas[59] caves from northeastern Morocco inland. Labels of archeological layers/units from the original references are indicated. The chronology of Moroccan archeological layers/units is given at probability level 65% (1σ).

Témara region have been roughly reported from other sites, such as Dar es Soltane 1,[55] Contrebandiers,[56] and El Harhoura 2[25] While some sequences revealed evidence of low Aterian hunter-gatherer settlements dated to MIS4-3, viz. Dar es Soltane 1,[55] El Harhoura 2,[54] and El Mnasra,[53] taphonomic analyses of faunal remains highlighted the predominance of non-human predator activities, unlike during MIS5[57] (Figure 3C). In summary, archaeological insights from coastal sites suggest long-term shifts in Aterian occupation densities with respect to paleoenvironmental changes (transition from interglacial-like, MIS5c and MIS5a, to glacial, MIS 4–3, global conditions), although nuances still exist and further studies are needed for more robust and highly resolved timeline constraints. While coastal sites might constitute wildlife refugia, outcomes from inland sequences are highly important.

Several dozens of kilometers far from the Mediterranean coast in northeastern Morocco, three MSA sites deliver more consistent insights into Aterian occupation phases: Ifri n'Ammar (Figure 3D), Taforalt (Figure 3E), and Ghafas (Figure 3F) caves (Figure S1). The three sites highlight an intense occupation centered

at ca. 80 ka BP,[21,59,61] coeval with that in Témara region. Besides Aterian culture markers (e.g., tanged pieces, bifacial foliates), the archaeological levels yield evidence of intense beadwork activities.[26,60] The use of *Nassarius* beads and associated pigments as personnel ornaments and symbolic cultural materials to convey coded information among AMH groups from coastal (e.g., Témara region) toward inland sites (northeastern Morocco) around 80 ka (MIS5a) is a strong hint of organized exchange networks.[26] The degree of this interconnection among remote groups decreased sharply after MIS5 as evidence of intense beadworking from the northeastern sites is not deliberately reported.[26] Instead, the extent of this innovation would be limited to coastal sites (Témara region) by that time. Accordingly, the archaeological findings, again, suggest striking shifts in Aterian behavioral traits and occupations in Morocco at the MIS5-4 transition as a result of the downstream effects of climate as supported by our paleoclimate data.

More regionally, according to the human dispersal model elaborated by Timmermann and Friedrich[15] to evaluate the number of individuals per 100 km^2 within NW Africa, a significant increase in human density coincides with the MIS5a Green Sahara period (Figure 3H). This is also suggested by the regional probability density function of archaeological sites[58] (Figure 3G) and with the reported Moroccan archaeological sequences (Figures 3B–3F). Afterward, a substantial decrease in human density coincides with the onset of dry conditions synchronous with HE7. This suggests that human populations contracted back into refuge areas after the Green Sahara declined during the MIS5-4 transition. By that time, climate and regional archaeological data suggest that the Sahara had largely expanded.[12] As such, our data support the close linkage between climate variability and human population in NW Africa, especially in Morocco. However, contrary to the common assumption that the Green Sahara was solely linked to the intensification of the summer African monsoon, we demonstrate that the favorable environmental conditions, and therefore the survival of early humans in this region, were also supported by winter precipitation associated with the westerlies. This is ostensibly supported by the intense human occupation during MIS5a in northeastern Morocco, an area far from the influence of the African monsoon.

While evidence of Aterian occupations is found in the northwestern Sahara, it is conceivable that the present desert might have played an important role in modern human dispersals. It has indeed been shown that the "Aterian" demographic changes are consistent with the Saharan paleoclimate from MIS6 to MIS5.[22] However, while the archaeological record reveals that the "Aterians" occupied a large area extending from the Mediterranean coast to the south of the Sahara, and from the Atlantic coast to the desert of Egypt, excluding the Nile Valley[62] (which is questioned by Scerri[19]), most of the currently dated "Aterian" sites are only limited to the Maghreb. To summarize, the consistency between the Wintimdouine cave record and paleoclimate evidence from the eastern part of North Africa (Figure 2) illustrates the significant and widespread impact of the retreat of the Green Sahara across North Africa during the MIS5-4 transition, which might have influenced the dynamics of local human. Indeed, the comparison of our new climate records with local and regional archaeological datasets reinforces our assumption about potential dispersals of NW African populations due to inhospitable environmental conditions after MIS5; human occupations would be limited to ecological refugia along coastal areas such as Témara region, or even possibly along the Nile in NE Africa, and a possible exodus out of Africa is likely through permanent corridors (e.g., coastlines). Nevertheless, due to the insufficient dating of Aterian sites in the Sahara, our findings are not conclusive about the Aterians that were present in the Maghreb during the same period. Hence, additional and improved chronometric evidence of archaeological sites is still needed in the Sahara in order to confirm whether the human populations that declined in NW Africa during the MIS5-4 transition correspond to Saharan "Aterians" or some other NW Saharan populations.

Conclusions

Despite the overwhelming evidence in favor of the Green Sahara periods, their moisture sources and northward extent remain unclear. Here, we presented a new multi-proxy speleothem record derived from three stalagmites from Wintimdouine cave in NW Africa (SW Morocco). The record documents two periods of increased precipitation lasting from 84 to 77 ka and from 9 to 4 ka BP, synchronous with the Green Sahara periods of MIS5a and the Early to Mid-Holocene, respectively. The consistency between our data and paleoclimate records from further south, as well as the Eastern Mediterranean and Eastern Africa, demonstrates the spatiotemporal extent of the Green Sahara during both periods. Our data also reveal abrupt millennial-scale climate change, indicative of a consistent climate forcing of the abrupt high-latitude temperature shifts during HEs HE8, HE7a, HE7b, and possibly HE1. Specifically, for MIS5a, this is an important result from the only paleoclimate record with absolute dating from NW Africa and highlights the extent of atmospheric linkage between the North African monsoon and the northern high-latitude temperature variations. Furthermore, the $\delta^{18}O$ and $\delta^{13}C$ combined with the

$\Delta^{17}O$ data points reveal a significant increase in winter precipitation in NW Africa during the Green Sahara period of MIS5a, whereas a major change in the source of moisture increased summer precipitation during the most recent Green Sahara period. The deterioration of climatic conditions between the end of MIS5 and the onset of MIS4 coincides with a sharp decline in human density in NW Africa during MIS4, a period when the Sahara Desert had already expanded. This is in line with paleoclimate and archaeological findings which document human dispersals and a possible exodus out of Africa as a response to inhospitable environmental conditions during the MIS5-4 transition.

Limitations of the study

The resolution of the Archaeological findings needs to be improved through more studies and chronological controls. In particular, more Aterian sites need to be dated, especially in the Sahara region. Furthermore, more research needs to be carried out to produce high-resolution paleoclimate records and their coupling with archaeological evidence and human dispersal models.

STAR★METHODS

Detailed methods are provided in the online version of this paper and include the following:

- KEY RESOURCES TABLE
- RESOURCE AVAILABILITY
  - Lead contact
  - Materials availability
  - Data and code availability
- EXPERIMENTAL MODEL AND SUBJECT DETAILS
- METHOD DETAILS
  - Samples and cave site
  - Mineral composition analysis
  - ^{230}Th dating method
  - Calcite stable isotope analysis
  - $\Delta^{17}O$ content of speleothem carbonates
  - Trace elements analysis
  - Interpretation of speleothem $\delta^{13}C$

SUPPLEMENTAL INFORMATION

Supplemental information can be found online at https://doi.org/10.1016/j.isci.2023.107018.

ACKNOWLEDGMENTS

This work was supported by grants from NSFC (4191101138), the Postdoctoral Science Foundation of China (2018M640971), the Hassan II Academy of Science and Technology (CHARISMA), and the Institute for Basic Science (IBS) under IBS-R028-Y2.

AUTHOR CONTRIBUTIONS

Y.A. designed the manuscript. Y.A. and L.S. performed the analytical work. Y.A., F.W., and L.B. carried out the field work. Y.A. coordinated this project. Y.A., L.S., J.W., K.A., H.C., F.W., and L.B. revised the manuscript.

DECLARATION OF INTERESTS

The authors declare no conflict of interest.

INCLUSION AND DIVERSITY

We support inclusive, diverse, and equitable conduct of research.

Received: October 11, 2022
Revised: March 19, 2023
Accepted: May 30, 2023
Published: June 7, 2023

REFERENCES

1. Sha, L., Ait Brahim, Y., Wassenburg, J.A., Yin, J., Peros, M., Cruz, F.W., Cai, Y., Li, H., Du, W., Zhang, H., et al. (2019). How far north did the african monsoon fringe expand during the african humid period? Insights from southwest Moroccan speleothems. Geophys. Res. Lett. *46*, 14093–14102. https://doi.org/10.1029/2019GL084879.

2. Tierney, J.E., Pausata, F.S.R., and deMenocal, P.B. (2017). Rainfall regimes of the green Sahara. Sci. Adv. *3*, e1601503. https://doi.org/10.1126/sciadv.1601503.

3. Pausata, F.S., Messori, G., and Zhang, Q. (2016). Impacts of dust reduction on the northward expansion of the African monsoon during the Green Sahara period. Earth Planet Sci. Lett. *434*, 298–307. https://doi.org/10.1016/j.epsl.2015.11.049.

4. Wagner, B., Vogel, H., Francke, A., Friedrich, T., Donders, T., Lacey, J.H., Leng, M.J., Regattieri, E., Sadori, L., Wilke, T., et al. (2019). Mediterranean winter rainfall in phase with African monsoons during the past 1.36 million years. Nature *573*, 256–260. https://doi.org/10.1038/s41586-019-1529-0.

5. Kutzbach, J.E., Guan, J., He, F., Cohen, A.S., Orland, I.J., and Chen, G. (2020). African climate response to orbital and glacial forcing in 140,000-y simulation with implications for early modern human environments. Proc. Natl. Acad. Sci. USA *117*, 2255–2264. https://doi.org/10.1073/pnas.1917673117.

6. Andersen, K.K., Azuma, N., Barnola, J.M., Bigler, M., Biscaye, P., Caillon, N., Chappellaz, J., Clausen, H.B., Dahl-Jensen, D., Fischer, H., et al. (2004). High-resolution record of Northern Hemisphere climate extending into the last interglacial period. Nature *431*, 147–151.

7. Weldeab, S., Lea, D.W., Schneider, R.R., and Andersen, N. (2007). 155,000 Years of West African monsoon and ocean thermal evolution. Science *316*, 1303–1307. https://doi.org/10.1126/science.1140461.

8. Stríkis, N.M., Cruz, F.W., Barreto, E.A.S., Naughton, F., Vuille, M., Cheng, H., Voelker, A.H.L., Zhang, H., Karmann, I., Edwards, R.L., et al. (2018). South American monsoon response to iceberg discharge in the North Atlantic. Proc. Natl. Acad. Sci. USA *115*, 3788–3793. https://doi.org/10.1073/pnas.1717784115.

9. Naughton, F., Sánchez Goñi, M., Kageyama, M., Bard, E., Duprat, J., Cortijo, E., Desprat, S., Malaizé, B., Joly, C., Rostek, F., and Turon, J.L. (2009). Wet to dry climatic trend in north-western Iberia within Heinrich events. Earth Planet Sci. Lett. *284*, 329–342. https://doi.org/10.1016/j.epsl.2009.05.001.

10. Skonieczny, C., McGee, D., Winckler, G., Bory, A., Bradtmiller, L.I., Kinsley, C.W., Polissar, P.J., De Pol-Holz, R., Rossignol, L., and Malaizé, B. (2019). Monsoon-driven Saharan dust variability over the past 240,000 years. Sci. Adv. *5*, eaav1887. https://doi.org/10.1126/sciadv.aav1887.

11. Skonieczny, C., Paillou, P., Bory, A., Bayon, G., Biscara, L., Crosta, X., Eynaud, F., Malaizé, B., Revel, M., Aleman, N., et al. (2015). African humid periods triggered the reactivation of a large river system in Western Sahara. Nat. Commun. *6*, 8751. https://doi.org/10.1038/ncomms9751.

12. Larrasoaña, J.C., Roberts, A.P., and Rohling, E.J. (2013). Dynamics of green Sahara periods and their role in hominin evolution. PLoS One *8*, e76514. https://doi.org/10.1371/journal.pone.0076514.

13. Pausata, F.S., Gaetani, M., Messori, G., Berg, A., Maia de Souza, D., Sage, R.F., and deMenocal, P.B. (2020). The greening of the Sahara: past changes and future implications. One Earth *2*, 235–250. https://doi.org/10.1016/j.oneear.2020.03.002.

14. Hublin, J.-J., Ben-Ncer, A., Bailey, S.E., Freidline, S.E., Neubauer, S., Skinner, M.M., Bergmann, I., Le Cabec, A., Benazzi, S., Harvati, K., and Gunz, P. (2017). New fossils from Jebel Irhoud, Morocco and the pan-African origin of Homo sapiens. Nature *546*, 289–292. https://doi.org/10.1038/nature22336.

15. Timmermann, A., and Friedrich, T. (2016). Late Pleistocene climate drivers of early human migration. Nature *538*, 92–95. https://doi.org/10.1038/nature19365.

16. Tierney, J.E., deMenocal, P.B., and Zander, P.D. (2017). A climatic context for the out-of-Africa migration. Geology *45*, 1023–1026. https://doi.org/10.1130/G39457.1.

17. Ziegler, M., Simon, M.H., Hall, I.R., Barker, S., Stringer, C., and Zahn, R. (2013). Development of Middle Stone Age innovation linked to rapid climate change. Nat. Commun. *4*, 1905. https://doi.org/10.1038/ncomms2897.

18. van de Loosdrecht, M., Bouzouggar, A., Humphrey, L., Posth, C., Barton, N., Aximu-Petri, A., Nickel, B., Nagel, S., Talbi, E.H., El Hajraoui, M.A., et al. (2018). Pleistocene North african genomes link near eastern and sub-saharan african human populations. Science *360*, 548–552. https://doi.org/10.1126/science.aar8380.

19. Scerri, E.M. (2013). The aterian and its place in the North African middle stone age. Quat. Int. *300*, 111–130. https://doi.org/10.1016/j.quaint.2012.09.008.

20. Dibble, H.L., Aldeias, V., Jacobs, Z., Olszewski, D.I., Rezek, Z., Lin, S.C., Alvarez-Fernández, E., Barshay-Szmidt, C.C., Hallett-Desguez, E., Reed, D., et al. (2013). On the industrial attributions of the aterian and mousterian of the Maghreb. J. Hum. Evol. *64*, 194–210. https://doi.org/10.1016/j.jhevol.2012.10.010.

21. Richter, D., Moser, J., Nami, M., Eiwanger, J., and Mikdad, A. (2010). New chronometric data from Ifri n'Ammar (Morocco) and the chronostratigraphy of the middle palaeolithic in the western Maghreb. J. Hum. Evol. *59*, 672–679. https://doi.org/10.1016/j.jhevol.2010.07.024.

22. Drake, N., and Breeze, P. (2016). Climate change and modern human occupation of the Sahara from MIS 6-2. In Africa from MIS 6-2: Population Dynamics and Paleoenvironments Vertebrate Paleobiology and Paleoanthropology, S.C. Jones and B.A. Stewart, eds. (Springer Netherlands), pp. 103–122. https://doi.org/10.1007/978-94-017-7520-5_6.

23. Linstädter, J., Eiwanger, J., Mikdad, A., and Weniger, G.-C. (2012). Human occupation of northwest Africa: a review of middle palaeolithic to epipalaeolithic sites in Morocco. Quat. Int. *274*, 158–174. https://doi.org/10.1016/j.quaint.2012.02.017.

24. Stoetzel, E., Campmas, E., Michel, P., Bougariane, B., Ouchaou, B., Amani, F., El Hajraoui, M.A., and Nespoulet, R. (2014). Context of modern human occupations in North Africa: contribution of the Témara caves data. Quat. Int. *320*, 143–161. https://doi.org/10.1016/j.quaint.2013.05.017.

25. Jacobs, Z., Roberts, R.G., Nespoulet, R., El Hajraoui, M.A., and Debénath, A. (2012). Single-grain OSL chronologies for middle palaeolithic deposits at El Mnasra and El Harhoura 2, Morocco: implications for late pleistocene human–environment interactions along the atlantic coast of northwest Africa. J. Hum. Evol. *62*, 377–394. https://doi.org/10.1016/j.jhevol.2011.12.001.

26. d'Errico, F., Vanhaeren, M., Barton, N., Bouzouggar, A., Mienis, H., Richter, D., Hublin, J.-J., McPherron, S.P., and Lozouet, P. (2009). Additional evidence on the use of personal ornaments in the middle paleolithic of North Africa. Proc. Natl. Acad. Sci. USA *106*, 16051–16056. https://doi.org/10.1073/pnas.0903532106.

27. Bar-Matthews, M., Marean, C.W., Jacobs, Z., Karkanas, P., Fisher, E.C., Herries, A.I., Brown, K., Williams, H.M., Bernatchez, J., Ayalon, A., and Nilssen, P.J. (2010). A high resolution and continuous isotopic speleothem record of paleoclimate and paleoenvironment from 90 to 53 ka from Pinnacle Point on the south coast of South Africa. Quat. Sci. Rev. *29*, 2131–2145. https://doi.org/10.1016/j.quascirev.2010.05.009.

28. Sha, L., Ait Brahim, Y., Wassenburg, J.A., Yin, J., Lu, J., Cruz, F.W., Cai, Y., Edwards, R.L., and Cheng, H. (2021). The "hockey stick" imprint in northwest African speleothems. Geophys. Res. Lett. *48*, e2021GL094232. https://doi.org/10.1029/2021GL094232.

29. Scholz, D., and Hoffmann, D.L. (2011). StalAge—an algorithm designed for construction of speleothem age models. Quat. Geochronol. *6*, 369–382. https://doi.org/10.1016/j.quageo.2011.02.002.

30. Ait Brahim, Y., Bouchaou, L., Sifeddine, A., Beraaouz, E.H., Wanaim, A., and Cheng, H. (2019). Hydro-climate characteristics of the karst system of Wintimdouine cave (Western High Atlas, Morocco): monitoring and implications for paleoclimate research. Environ. Earth Sci. *78*, 508. https://doi.org/10.1007/s12665-019-8496-5.

31. Ait Brahim, Y., Cheng, H., Sifeddine, A., Wassenburg, J.A., Cruz, F.W., Khodri, M., Sha, L., Pérez-Zanón, N., Beraaouz, E.H., Apaéstegui, J., et al. (2017). Speleothem records decadal to multidecadal hydroclimate variations in southwestern Morocco during the last millennium. Earth Planet Sci. Lett. *476*, 1–10. https://doi.org/10.1016/j.epsl.2017.07.045.

32. Ait Brahim, Y., Bouchaou, L., Sifeddine, A., Khodri, M., Reichert, B., and Cruz, F.W. (2016). Elucidating the climate and topographic controls on stable isotope composition of meteoric waters in Morocco, using station-based and spatially-interpolated data. J. Hydrol. X. *543*, 305–315. https://doi.org/10.1016/j.jhydrol.2016.10.001.

33. Berger, A., and Loutre, M.F. (1991). Insolation values for the climate of the last 10 million years. Quat. Sci. Rev. *10*, 297–317. https://doi.org/10.1016/0277-3791(91)90033-Q.

34. Wulf, S., Hardiman, M.J., Staff, R.A., Koutsodendris, A., Appelt, O., Blockley, S.P., Lowe, J.J., Manning, C.J., Ottolini, L., Schmitt, A.K., et al. (2018). The marine isotope stage 1–5 cryptotephra record of Tenaghi Philippon, Greece: towards a detailed tephrostratigraphic framework for the Eastern Mediterranean region. Quat. Sci. Rev. *186*, 236–262. https://doi.org/10.1016/j.quascirev.2018.03.011.

35. Pickarski, N., Kwiecien, O., Langgut, D., and Litt, T. (2015). Abrupt climate and vegetation variability of eastern Anatolia during the last glacial. Clim. Past *11*, 1491–1505. https://doi.org/10.5194/cp-11-1491-2015.

36. Langgut, D. (2018). Late quaternary nile flows as recorded in the levantine basin: the palynological evidence. Quat. Int. *464*, 273–284. https://doi.org/10.1016/j.quaint.2017.07.006.

37. Duplessy, J.C., Roche, D.M., and Kageyama, M. (2007). The deep ocean during the last interglacial period. Science *316*, 89–91. https://doi.org/10.1126/science.1138582.

38. Grant, K.M., Rohling, E.J., Bar-Matthews, M., Ayalon, A., Medina-Elizalde, M., Ramsey, C.B., Satow, C., and Roberts, A.P. (2012). Rapid coupling between ice volume and polar temperature over the past 150,000 years. Nature *491*, 744–747. https://doi.org/10.1038/nature11593.

39. Menviel, L., Timmermann, A., Friedrich, T., and England, M.H. (2014). Hindcasting the continuum of Dansgaard–Oeschger variability: mechanisms, patterns and timing. Clim. Past *10*, 63–77. https://doi.org/10.5194/cp-10-63-2014.

40. Timmermann, A., Friedrich, T., Timm, O.E., Chikamoto, M.O., Abe-Ouchi, A., and Ganopolski, A. (2014). Modeling obliquity and CO2 effects on southern hemisphere climate during the past 408 ka. J. Clim. *27*, 1863–1875. https://doi.org/10.1175/JCLI-D-13-00311.1.

41. Johnston, V.E., Borsato, A., Spötl, C., Frisia, S., and Miorandi, R. (2013). Stable isotopes in caves over altitudinal gradients: fractionation behaviour and inferences for speleothem sensitivity to climate change. Clim. Past *9*, 99–118. https://doi.org/10.5194/cp-9-99-2013.

42. Genty, D., Blamart, D., Ouahdi, R., Gilmour, M., Baker, A., Jouzel, J., and Van-Exter, S. (2003). Precise dating of Dansgaard–Oeschger climate oscillations in western Europe from stalagmite data. Nature *421*, 833–837. https://doi.org/10.1038/nature01391.

43. Castañeda, I.S., Mulitza, S., Schefuß, E., Lopes dos Santos, R.A., Sinninghe Damsté, J.S., and Schouten, S. (2009). Wet phases in the Sahara/Sahel region and human migration patterns in North Africa. Proc. Natl. Acad. Sci. USA *106*, 20159–20163. https://doi.org/10.1073/pnas.0905771106.

44. deMenocal, P.B., and Stringer, C. (2016). Climate and the peopling of the world. Nature *538*, 49–50. https://doi.org/10.1038/nature19471.

45. Haug, G.H., Hughen, K.A., Sigman, D.M., Peterson, L.C., and Röhl, U. (2001). Southward migration of the intertropical convergence zone through the Holocene. Science *293*, 1304–1308. https://doi.org/10.1126/science.1059725.

46. Deplazes, G., Lückge, A., Peterson, L.C., Timmermann, A., Hamann, Y., Hughen, K.A., Röhl, U., Laj, C., Cane, M.A., Sigman, D.M., and Haug, G.H. (2013). Links between tropical rainfall and North Atlantic climate during the last glacial period. Nat. Geosci. *6*, 213–217. https://doi.org/10.1038/ngeo1712.

47. Tjallingii, R., Claussen, M., Stuut, J.-B.W., Fohlmeister, J., Jahn, A., Bickert, T., Lamy, F., and Röhl, U. (2008). Coherent high- and low-latitude control of the northwest African hydrological balance. Nat. Geosci. *1*, 670–675. https://doi.org/10.1038/ngeo289.

48. Hoffmann, D.L., Rogerson, M., Spötl, C., Luetscher, M., Vance, D., Osborne, A.H., Fello, N.M., and Moseley, G.E. (2016). Timing and causes of North African wet phases during the last glacial period and implications for modern human migration. Sci. Rep. *6*, 36367. https://doi.org/10.1038/srep36367.

49. Rogerson, M., Dublyansky, Y., Hoffmann, D.L., Luetscher, M., Töchterle, P., and Spötl, C. (2019). Enhanced Mediterranean water cycle explains increased humidity during MIS 3 in North Africa. Clim. Past *15*, 1757–1769. https://doi.org/10.5194/cp-15-1757-2019.

50. Ait Brahim, Y., Wassenburg, J.A., Sha, L., Cruz, F.W., Deininger, M., Sifeddine, A., Bouchaou, L., Spötl, C., Edwards, R.L., and Cheng, H. (2019). North Atlantic ice-rafting, ocean and atmospheric circulation during the Holocene: insights from western mediterranean speleothems. Geophys. Res. Lett. *46*, 7614–7623.

51. Boch, R., Cheng, H., Spötl, C., Edwards, R.L., Wang, X., and Häuselmann, P. (2011). NALPS: a precisely dated European climate record 120–60 ka. Clim. Past *7*, 1247–1259. https://doi.org/10.5194/cp-7-1247-2011.

52. Budsky, A., Wassenburg, J.A., Mertz-Kraus, R., Spötl, C., Jochum, K.P., Gibert, L., and Scholz, D. (2019). Western mediterranean climate response to dansgaard/oeschger events: new insights from speleothem records. Geophys. Res. Lett. *46*, 9042–9053. https://doi.org/10.1029/2019GL084009.

53. Ben Arous, E., Philippe, A., Shao, Q., Richter, D., Lenoble, A., Mercier, N., Richard, M., Stoetzel, E., Tombret, O., El Hajraoui, M.A., et al. (2022). An improved chronology for the middle stone age at El Mnasra cave, Morocco. PLoS One *17*, e0261282. https://doi.org/10.1371/journal.pone.0261282.

54. Ben Arous, E., Falguères, C., Tombret, O., El Hajraoui, M.A., and Nespoulet, R. (2020). Combined US-ESR dating of fossil teeth from El Harhoura 2 cave (Morocco): new data about the end of the MSA in Temara region. Quat. Int. *556*, 58–65. https://doi.org/10.1016/j.quaint.2019.02.029.

55. Barton, R.N.E., Bouzouggar, A., Collcutt, S.N., Schwenninger, J.-L., and Clark-Balzan, L. (2009). OSL dating of the Aterian levels at Dar es-Soltan I (Rabat, Morocco) and implications for the dispersal of modern Homo sapiens. Quat. Sci. Rev. *28*, 1914–1931. https://doi.org/10.1016/j.quascirev.2009.03.010.

56. Jacobs, Z., Meyer, M.C., Roberts, R.G., Aldeias, V., Dibble, H., and El Hajraoui, M.A. (2011). Single-grain OSL dating at La Grotte des Contrebandiers ('Smugglers' Cave'), Morocco: improved age constraints for the Middle Paleolithic levels. J. Archaeol. Sci. *38*, 3631–3643. https://doi.org/10.1016/j.jas.2011.08.033.

57. Campmas, E., Michel, P., Costamagno, S., Amani, F., Stoetzel, E., Nespoulet, R., and El Hajraoui, M.A. (2015). Were Upper Pleistocene human/non-human predator occupations at the Témara caves (El Harhoura 2 and El Mnasra, Morocco) influenced by climate change? J. Hum. Evol. *78*, 122–143. https://doi.org/10.1016/j.jhevol.2014.08.008.

58. Scerri, E.M.L. (2017). The North african middle stone age and its place in recent human evolution. Evol. Anthropol. *26*, 119–135. https://doi.org/10.1002/evan.21527.

59. Doerschner, N., Fitzsimmons, K.E., Ditchfield, P., McLaren, S.J., Steele, T.E., Zielhofer, C., McPherron, S.P., Bouzouggar, A., and Hublin, J.-J. (2016). A new chronology for rhafas, northeast Morocco, spanning the North African middle stone age through to the neolithic. PLoS One *11*, e0162280. https://doi.org/10.1371/journal.pone.0162280.

60. Bouzouggar, A., Barton, N., Vanhaeren, M., d'Errico, F., Collcutt, S., Higham, T., Hodge, E., Parfitt, S., Rhodes, E., Schwenninger, J.-L., et al. (2007). 82,000-year-old shell beads from North Africa and implications for the origins of modern human behavior. Proc. Natl. Acad. Sci. USA *104*, 9964–9969. https://doi.org/10.1073/pnas.0703877104.

61. Clark-Balzan, L.A., Candy, I., Schwenninger, J.-L., Bouzouggar, A., Blockley, S., Nathan, R.,

and Barton, R.N.E. (2012). Coupled U-series and OSL dating of a late pleistocene cave sediment sequence, Morocco, North Africa: significance for constructing palaeolithic chronologies. Quat. Geochronol. *12*, 53–64. https://doi.org/10.1016/j.quageo.2012.06.006.

62. Hublin, J.-J., Verna, C., Bailey, S., Smith, T., Olejniczak, A., Sbihi-Alaoui, F.Z., and Zouak, M. (2012). Dental evidence from the aterian human populations of Morocco. In Modern Origins: A North African Perspective Vertebrate Paleobiology and Paleoanthropology, J.-J. Hublin and S.P. McPherron, eds. (Springer Netherlands), pp. 189–204. https://doi.org/10.1007/978-94-007-2929-2_13.

63. Sha, L., Mahata, S., Duan, P., Luz, B., Zhang, P., Baker, J., Zong, B., Ning, Y., Brahim, Y.A., Zhang, H., et al. (2020). A novel application of triple oxygen isotope ratios of speleothems. Geochem. Cosmochim. Acta *270*, 360–378. https://doi.org/10.1016/j.gca.2019.12.003.

64. Paul, D., Skrzypek, G., and Fórizs, I. (2007). Normalization of measured stable isotopic compositions to isotope reference scales – a review. Rapid Commun. Mass Spectrom. *21*, 3006–3014. https://doi.org/10.1002/rcm.3185.

65. Barkan, E., Affek, H.P., Luz, B., Bergel, S.J., Voarintsoa, N.R.G., and Musan, I. (2019). Calibration of δ17O and 17Oexcess values of three international standards: IAEA-603, NBS19 and NBS18. Rapid Commun. Mass Spectrom. *33*, 737–740. https://doi.org/10.1002/rcm.8391.

66. Fairchild, I.J., Borsato, A., Tooth, A.F., Frisia, S., Hawkesworth, C.J., Huang, Y., McDermott, F., and Spiro, B. (2000). Controls on trace element (Sr–Mg) compositions of carbonate cave waters: implications for speleothem climatic records. Chem. Geol. *166*, 255–269. https://doi.org/10.1016/S0009-2541(99)00216-8.

STAR★METHODS

KEY RESOURCES TABLE

REAGENT or RESOURCE	SOURCE	IDENTIFIER
Software and algorithms		
StalAge algorithm	Scholz and Hoffmann (2011)[29]	https://doi.org/10.1016/j.quageo.2011.02.002
Other		
Shimadzu XRD 7000	Frontier Institute of Science and Technology (Xi'an Jiaotong University)	http://fist.xjtu.edu.cn/en/index.htm
Neptune Plus MC-ICPMS	Isotope Laboratory of Xi'an Jiaotong University (China)	http://isotope.xjtu.edu.cn/jjy.jsp?urltype=tree.TreeTempUrl&wbtreeid=1019
Isotope-Ratio Mass Spectrometry	Isotope Laboratory of Xi'an Jiaotong University	http://isotope.xjtu.edu.cn/jjy.jsp?urltype=tree.TreeTempUrl&wbtreeid=1019
O_2-CO_2 Pt-catalyzed oxygen isotope equilibrium	Isotope Laboratory of Xi'an Jiaotong University	http://isotope.xjtu.edu.cn/jjy.jsp?urltype=tree.TreeTempUrl&wbtreeid=1019
Laser-Induced Breakdown Spectroscopy (LIBS)	Isotope Laboratory of Xi'an Jiaotong University	http://isotope.xjtu.edu.cn/jjy.jsp?urltype=tree.TreeTempUrl&wbtreeid=1019

RESOURCE AVAILABILITY

Lead contact

Further information and requests for resources should be directed to and will be fulfilled by the lead contact, Yassine Ait Brahim (yassine.aitbrahim@um6p.ma).

Materials availability

All newly created databases from this study can be found in Supplementary Materials.

Data and code availability

- The data produced in this study can be downloaded via the NOAA Paleoclimate Database using this link: https://www.ncei.noaa.gov/access/paleo-search/study/38081
- This paper does not report original code.
- For any further inquiries or additional information required to reanalyze the data reported in this paper, please contact the lead author.

EXPERIMENTAL MODEL AND SUBJECT DETAILS

Our study does not use experimental models.

METHOD DETAILS

Samples and cave site

Wintimdouine cave is developed within the karst system of Tasroukht in the Western High Atlas Mountains in SW Morocco[30] (Figure S1). The rainy season in the cave region is from October to April with the highest rainfall amounts from December to February. Three stalagmites, WIN1, WIN3, and WIN15 (197, 285, and 300 mm long respectively) were collected from Wintimdouine cave in 2010. The stalagmites were halved and polished (Figure S2).

Mineral composition analysis

The mineral composition of the stalagmites was analyzed with X-ray diffraction using a Shimadzu XRD 7000 at the Frontier Institute of Science and Technology of Xi'an Jiaotong University. The results indicate that the three stalagmites are composed of calcite.

^{230}Th dating method

A total of 10, 34 and 21 ^{230}Th dates were obtained from the stalagmites WIN1, WIN3, and WIN15 respectively. The ^{230}Th dating was performed at the Isotope Laboratory of Xi'an Jiaotong University (China) using a Neptune Plus Multi-Collector Inductively Coupled Plasma Mass Spectrometry (MC-ICPMS). Ages are reported in kilo years before the present (ka BP) with 1950 AD as the year of reference.

Calcite stable isotope analysis

Calcite subsamples were drilled and milled using a MicroMill from the growth axis of each stalagmite with a spatial resolution of 0.1, 1 and 0.5 mm from the stalagmites WIN1, WIN3 and WIN15, respectively. Hence, a total of 44, 1570 and 315 calcite subsamples were collected from the stalagmites WIN1, WIN3 and WIN15 respectively. Isotope-Ratio Mass Spectrometry was used to measure the calcite oxygen and carbon stable isotopes ($\delta^{18}O$ and $\delta^{13}C$) at the Isotope Laboratory of Xi'an Jiaotong University. Results were reported relative to the Vienna Pee Dee Belemnite (VPDB) standard with an analytical error of less than 0.1‰.

$\Delta^{17}O$ content of speleothem carbonates

Nine calcite samples were drilled from the stalagmite WIN1, WIN3 and WIN15 in order to precisely measure the $\delta^{17}O$ and $\Delta^{17}O$ values of their CO_2, using the O_2-CO_2 Pt-catalyzed oxygen isotope equilibrium. The method we used was developed by Sha et al.,[63] who showed that modern paired ^{17}O-excess (drip water) and $\Delta^{17}O$ (speleothem carbonate) data can be interpreted as a relative humidity proxy at the moisture source.

The major steps that were used include (i) extraction of CO_2 gas from carbonates by using concentrated phosphoric acid at 25°C; (ii) the equilibration of the extracted CO_2 and O_2 with known isotope composition for 30 minutes under Pt-catalyzation at 750°C; (iii) cryogenic separation of two post-equilibration gases; (iv) Finally, the measurement of the equilibrated O_2 using a MAT-253 Stable Isotope Ratio Mass Spectrometer, and the calculation of the $\delta^{17}O$ and $\Delta^{17}O$ values of the CO_2 extracted from speleothem carbonates. The $\delta^{18}O$ values of the CO_2 standard gases were directly measured and normalized to concurrent analyses of NBS18, which were then cross-calibrated to another standard IEAE603. To normalize the measured $\delta^{17}O$ values, we applied a two-point linear normalization method,[64] using high-precision values of standards NBS18 and IAEA603, respectively.[65] The normalization was only applied to the measured $\delta^{17}O$ value. The normalized $\delta^{17}O$ value was used to calculate $\Delta^{17}O$.

Trace elements analysis

Trace element measurements (Mg/Ca and Sr/Ca) were made at the Isotope Laboratory of Xi'an Jiaotong University using the Laser-Induced Breakdown Spectroscopy (LIBS) technique. The laser beam was focused onto the stalagmite's surface with a 50 mm focal-distance lens. The emitted plasma was collected and then focused into an optical fiber (2-meter length, 600 μm core diameter, 0.22 numerical aperture) coupled to a spectrometer (Ocean Optics MX500+). The spectral resolution of the spectrometer system in which the wavelength ranged from 200 to 580 nm was 0.1 nm. Each sampling point was exposed to 5 laser shots before performing the measurements in order to pre-clean the surface. Analyses were conducted by pulsing the laser to measure trace elements on every point in 0.3-mm increments along the growth axis of stalagmite WIN15. The recorded spectra were the average of 20 laser pulses at every single position.

Interpretation of speleothem $\delta^{13}C$

Prior calcite precipitation is a process that occurs when infiltrated water encounters air-filled voids within the karst aquifer that have a lower partial CO_2 pressure compared to the water itself. This causes CO_2 degassing and drives the water to a supersaturated state with respect to $CaCO_3$ and thus calcite precipitation.[66] Because the volume of air in the karst aquifer increases with decreasing water infiltration, prior calcite precipitation is usually linked to the amount of rainfall or more precisely the precipitation-evaporation balance. When calcite precipitates within the karst aquifer it increases the $\delta^{13}C$ value of the dissolved inorganic carbon. Prior calcite precipitation also affects Mg/Ca and Sr/Ca ratios of the water because calcite prefers to incorporate Ca over Mg and Sr.[66] An increase in speleothem $\delta^{13}C$, Mg/Ca and Sr/Ca ratios are thus often interpreted as a relatively dry climate. In the case of the WIN15 speleothem record it is clear that not all variations that we observe in Mg/Ca, Sr/Ca and $\delta^{13}C$ can be explained by prior calcite precipitation. Nevertheless, the strong positive correlations of these three parameters with the first principal component of the principal component analysis (Tables S2 and S3) strongly suggest that prior calcite

precipitation is one of the dominant processes affecting WIN15 $\delta^{13}C$. The even stronger response of WIN15 $\delta^{13}C$ to Heinrich events compared to Mg/Ca and Sr/Ca also implies that vegetation productivity and soil activity may have reinforced the prior calcite precipitation signal. Because vegetation and soil activity is highly dependent on soil moisture and temperature.[42] A decrease in soil moisture and cooler temperatures results in lower vegetation productivity and lower soil activity, which leads to higher $\delta^{13}C$ values in soil CO_2, ultimately leading to higher speleothem $\delta^{13}C$.